

fractionated RT (12). For conventional fractionated RT, the relationship between lung dose and RP has been extensively evaluated (*e.g.*, ref. 13). RP is a serious complication after irradiation, and fatal RP toxicities are also observed after hypofractionated schemes (14).

To evaluate the applicability of the LQ(L) model and normal tissue complication models for higher-dose per fraction, we evaluated the prediction of RP occurring after hypofractionated RT. Different α/β ratios and different d_T values of the LQ(L) models were analyzed, modeling the probability of RP after hypofractionated RT as function of the dose.

METHODS AND MATERIALS

Patients

Patients and treatment schedules were comprehensively described elsewhere (12). In summary, 128 patients were irradiated with hypofractionated RT at the Department of Radiation Medicine of the Hokkaido University School of Medicine, Sapporo, Japan, with 35 Gy in 4 fractions, 40 Gy in 4 fractions, 48 Gy in 8 fractions, 60 Gy in 8 fractions, and 48 Gy in 4 fractions. Twenty patients had multiple targets in one treatment plan (18 patients had two targets, 2 patients had three targets). For 13 patients, multiple treatment plans were made for different targets because of metastasis or recurrence (5 patients had two plans, 4 patients had three plans, and 4 patients had four plans) (for time schedule, dose schedule, and tolerated maximum dose for organs at risk see ref. 12).

Toxicity

RP was prospectively scored according to National Cancer Institute Common Toxicity Criteria (NCI-CTC) version 2, in which grade 2 RP is scored after prescribing steroids for treatment-related toxicity, like progressive shortness of breath combined with typical RP changes on the X-thorax. Grade 3 RP is scored after requiring oxygen. None of the patients whose RP was grade 2 had used steroids before radiotherapy. For all patients, the diagnosis and grade of RP were determined by a radiation oncologist and a pulmonologist experienced in the diagnosis of RP. Patients for whom the diagnosis of RP was unlikely were not included (those with progressive cardiac problems, medical history of receiving oxygen before treatment, and tumor progression).

Dose

Three dimensional treatment plans were made using Focus (CMS, St. Louis, MO), XiO (CMS), or Pinnacle. A convolution superposition algorithm for tissue density heterogeneity was used (plans initially carried out with the Clarkson method were recalculated). Normal lung tissue was defined by computed tomography scan by binary thresholding (thus, excluding the gross tumor volume). Both lungs were considered together as one organ. Four to six noncoplanar beams were used. The beam energy was 4, 6, or 10 MV. Plans were further analyzed with in-house-developed software. The physical dose distribution was converted into the normalized total dose (NTD) distribution (15), using the LQ model. The NTD is defined as the equivalent total dose given in fractions of 2 Gy, as follows:

$$\text{NTD} = D \frac{d + \alpha/\beta}{2 + \alpha/\beta} \quad (1)$$

in which the total dose (D) is the number of fractions multiplied by the dose per fraction (d).

Dose distributions were converted according to Eq. 1 (1) for α/β ratios of 1 Gy, 2 Gy, 3 Gy, 4 Gy, 5 Gy, 7.5 Gy, 10 Gy, and infinity (*i.e.*, physical dose) to evaluate the effect of different α/β ratios. After this conversion for the dose per fraction, we determined different dose-volume parameters from the dose-volume histograms: the mean lung dose (MLD) and the lung volume percentage receiving doses higher than 5 Gy (V_5), 13 Gy (V_{13}), 20 Gy (V_{20}), 40 Gy (V_{40}), and 50 Gy (V_{50}) or, in general, higher than x Gy (V_x). For the 33 patients who underwent irradiation for multiple lesions, individual plans were summed after NTD corrections, and image registration had been performed. Time-related recovery of lung tissue was not taken into account for multiple treatments.

The dose response relationship between RP and MLD was modeled by a sigmoid-shaped dose effect relationship according to Lyman (16). The NTCP can be calculated from the MLD (17) according to the equation:

$$\text{NTCP} = \frac{1}{\sqrt{2\pi}} \int_{-\infty}^t e^{-x^2/2} dx \quad (2)$$

with $t = \frac{\text{MLD} - \text{TD}_{50}}{m - \text{TD}_{50}}$ in which TD_{50} represents the dose for a 50% NTCP and m is the (inverse) steepness parameter in the standard formulation of the Lyman model. Similarly for the V_x parameter, Eq. 2 was used with $t = \frac{V_x - V_{x,50}}{m - V_{x,50}}$ such that the $V_{x,50}$ represents the V_x parameter for a 50% NTCP.

Modification of the LQ model to the LQL model

We adapted the LQ model (LQL) by applying a two-component model proposed by Park *et al.* (4) (Fig. 1). For the low-dose range, the total dose is corrected according to the LQ model by using Eq. 1 according to the best α/β ratio. For the high-dose range, the log survival curve is assumed to be linear. The slope of the linear part is determined by the derivative of the LQ curve at the cut-off value between the linear-quadratic part and the linear part (*i.e.*, the transition dose [d_T]) (Fig. 1, also see Appendix E1) resulting in the equation:

$$\text{NTD} = D \frac{\alpha/\beta + 2d_T - \frac{d_T^2}{d}}{2 + \alpha/\beta} \quad (3)$$

In contrast to nomenclature in the literature, we propose to use the denotation of a lower-case letter (d_T) because this transition dose refers to the dose-per-fraction correction. We converted the dose distributions for d_T values of 0 Gy, 5 Gy, 7 Gy, and 9 Gy and subsequently calculated the MLD (not the V_x) from these dose distributions (*i.e.*, MLDLQL).

Statistics

The terms TD_{50} and m were estimated by maximizing the logarithm of the likelihood function (17), as follows:

$$\begin{aligned} \ln(L) &= \ln\left(\prod_{i=1}^N L_i\right) = \sum_{i=1}^N \ln(L_i) \\ &= \sum_{i=1}^N [\text{ep}_i \ln(P_i) + (1 - \text{ep}_i) \ln(1 - P_i)] \end{aligned} \quad (4)$$

where P_i ($i = 1, \dots, N$) represents the predicted NTCP and ep_i is the observed binary outcome (0 = an RP grade of ≤ 1 , and 1 = an RP grade of ≥ 2) for patient i .

The confidence intervals (CI) of the fitted parameters were calculated using the profile likelihood method (18). These CI were

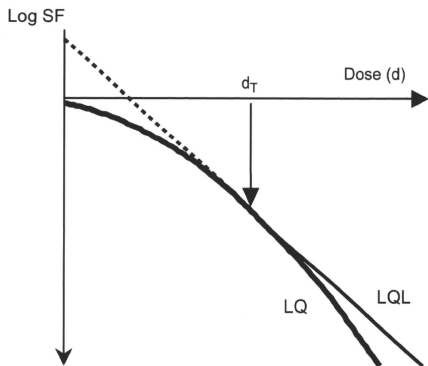


Fig. 1. Schematic representation of the log survival curve as a function of the dose according to the LQ model is shown. Below the transition dose (d_T), the curve is linear quadratic (the LQ model). Above d_T , the log survival curve is linear, whereby the slope is determined by the asymptote of the LQ model at dose d_T .

calculated by finding the points in the parameter space where the $\ln(L)$ values are $\Delta\ln(L)$ lower than $\ln(L_{\max})$ (e.g., for the 95% CI the value of $\Delta\ln(L)$ is 1.92, corresponding to half of the 95% percentile of the cumulative chi-square value for 1 degree of freedom).

In order to evaluate which α/β ratio would give the maximum likelihood estimation, a profile likelihood approach of the best NTCP fit was performed according to α/β ratios in the range of 1 Gy to infinity. This analysis was performed only for the MLD (i.e., the corrected mean lung dose [MLDLQ]).

Converting the dose according to the LQL model, we used an α/β ratio of 3 Gy. The LQ and the LQL models are nested, since the three-parameter (TD_{50} , m , and d_T) MLDLQL model reduces to the two-parameter (TD_{50} , m) MLDLQ model when d_T goes to infinity (or at least becomes higher than the highest dose-per-fraction value in the data set) (Fig. 1). According to the LQL model, the doses were converted with d_T values of 0, 5, 7, and 9 Gy. The NTCP model fit using the MLDLQL was compared to the NTCP model fit with the MLDLQ, using the maximum likelihood ratio test, since the two models were nested (19). For this analysis, this requires that twice the difference of the log likelihoods between the two models should be larger than the quantile of a chi-square distribution with 1 degree of freedom (i.e., 3.84/2) to be significantly different.

For regression analysis, the slope of the linear regression(s) with zero intercept was used to assess the relationship between different parameters. A two-tailed p value of <0.05 was considered to be statistically significant.

RESULTS

The crude incidence of RP was 10.9% (14 events in the group of 128 patients). One patient was diagnosed with a grade 3 RP, all other patients were diagnosed with grade 2 RP.

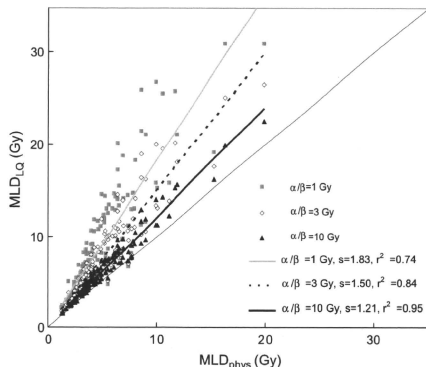


Fig. 2. The MLDLQ calculated according to the LQ model with α/β ratios of 1 Gy, 3 Gy, 10 Gy plotted as function of the MLD_{phys} . The straight line with a slope of 1 represents the equality line where $MLDLQ$ equals MLD_{phys} . The other lines represent the best fit through the data with a zero intercept; s represents the slope and r the regression coefficient.

MLD corrected for different α/β ratios

The relationships between the MLD calculated with an α/β ratio of infinity (MLD_{phys}) and of 1 Gy (MLD_1), 3 Gy (MLD_3), and 10 Gy (MLD_{10}) are illustrated in Fig. 2. The MLDLQ calculated with a low α/β ratio is higher than the MLDLQ calculated with a higher α/β ratio, as expected. A linear fit of the data (with zero intercept) resulted in the following relationships and correlations; $MLD_1 = 1.83 \times MLD_{\text{phys}}$ ($r^2 = 0.74$), $MLD_3 = 1.50 \times MLD_{\text{phys}}$ ($r^2 = 0.84$), and $MLD_{10} = 1.21 \times MLD_{\text{phys}}$ ($r^2 = 0.95$), respectively. Two patients were located under the equality line. These two patients were also irradiated at a target in the mediastinum with a more fractionated scheme whereby the high-dose region in the lung tissue received less than 2 Gy.

To evaluate the effect of the dose per fraction, the MLD_1 and the MLD_3 values were plotted as a function of the MLD_{phys} (Fig. 3) for each dose per fraction separately for patients irradiated on one single target. Because only 3 patients received 35 Gy/4 fractions, these patients were excluded. As expected, the slopes of the linear regression of the higher dose per fraction schedules (10 Gy and 12 Gy per fraction) were higher than for the lower dose per fraction schedules (6 Gy and 7.5 Gy per fraction). In addition, the slopes for the α/β ratio of 1 Gy was higher than the slope for the α/β ratio of 3 Gy for each dose per fraction. All correlations were significant with a p of <0.001 .

The MLD calculated according to the LQL model (MLDLQL) with a d_T of 5 Gy is shown as a function of the MLD_3 in Fig. 4. For patients with a high MLD_3 and who were irradiated with a high dose per fraction, larger differences between the MLD_3 and the MLDLQL were observed than for other patients (Fig. 4).

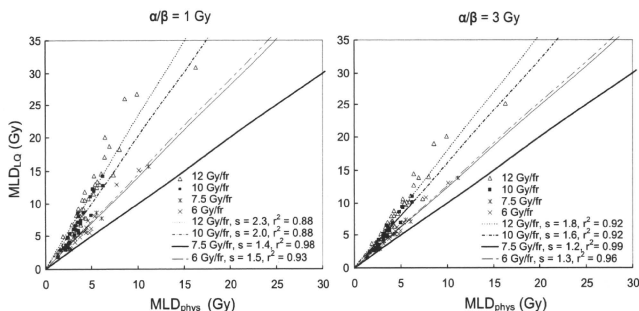


Fig. 3. The MLD_1 and MLD_3 as a function of the MLD_{phys} are plotted for different fractionation schemes. The straight line with a slope of 1 represents the equivalent line where MLD_{LQ} equals MLD_{phys} . The other lines represent the best fit through the data with a zero intercept; s represents the slope and r the regression coefficient.

NTCP for different α/β ratios and the LQ and V_x models

Optimizing the LQ NTCP model as a function of the m , TD_{50} , and α/β ratio revealed that the highest maximum log likelihood was found at an α/β ratio of 3 Gy (with $TD_{50} = 20.8$ Gy and $m = 0.45$). All other evaluated α/β ratios had lower maximum log likelihoods (Fig. 5) but were within the 95% CI of the NTCP fit with an α/β ratio of 3 Gy. The largest difference was found between the NTCP fit with an α/β ratio of 3 Gy and the NTCP fit with an α/β ratio of infinity (*i.e.*, physical dose) (with $TD_{50} = 14.6$ Gy, and $m = 0.48$), but this was not significant ($p = 0.07$) (Fig. 6).

Evaluating the NTCP model according to the LQL model with a d_T value of 5 Gy, the maximum log likelihood was lower than the MLD_3 NTCP LQ model fit. The LQL NTCP fit parameters TD_{50} of 19.5 Gy and $m = 0.46$ were not significantly different from the LQ fit parameters

($p = 0.28$). The NTCP model according to the LQL model with a d_T of 7 Gy and a d_T value of 9 Gy was approaching the MLD_3 NTCP LQ model fit, as expected, because only a limited part of the distribution of doses per fraction was larger than these d_T values. The NTCP according to the LQL model with a d_T value of 0 Gy was, as expected, similar to the MLD_{phys} NTCP LQ model fit.

For the V_x (calculated with the LQ model with an α/β ratio of 3 Gy), the maximum likelihood profile approach revealed that the highest likelihood (*i.e.*, best fit) is achieved with a threshold dose of 50 Gy. The V_{50} calculated with the LQL model had lower log likelihood parameters (worse fits), although these differences were not significant ($p = 0.16$ for $d_T = 5$ Gy and $p = 0.21$ for $d_T = 7$ Gy). For all other V_x values, similar results were observed (data not shown).

The values V_5 , V_{13} , and V_{20} were outside the 95% CI of V_{50} (Table 1). Because one patient had 0% of the lung volume receiving doses higher than 60 Gy (corrected for an α/β ratio of 3 Gy), we did not evaluate V_x values higher than 50 Gy.

DISCUSSION

Our results showed that the NTD-corrected MLD_{LQ} calculated with an α/β ratio of 3 Gy was the best parameter to fit the NTCP model to the observed incidence of RP after hypofractionated RT. These data suggest that a correction for the dose per fraction after hypofractionated radiotherapy should be performed similar to conventional fractionated schemes (*i.e.*, LQ model and an α/β ratio of 3 Gy [*e.g.*, see ref. 20]). Other tested α/β ratios or a modification of the LQ model (by introducing a linear relation after a threshold dose d_T of 5 Gy or higher) deteriorated the predictive value of the lung dose but were within the 95% CI of the NTCP LQ model fit with an α/β ratio of 3 Gy. The nonsignificant differences in the NTCP fits might be explained by the strong correlations between the corrected dose parameters.

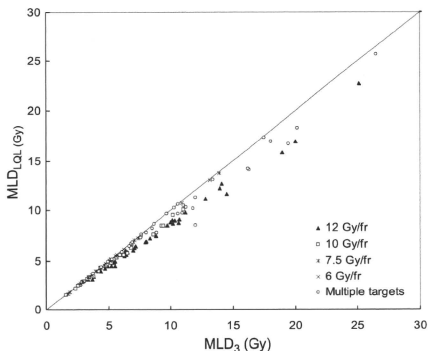


Fig. 4. The MLD_{LQ} as a function of MLD_3 is shown plotted for different fractionation schemes. The straight line with a slope 1 represents the equivalent line where MLD_{LQ} equals MLD_3 .

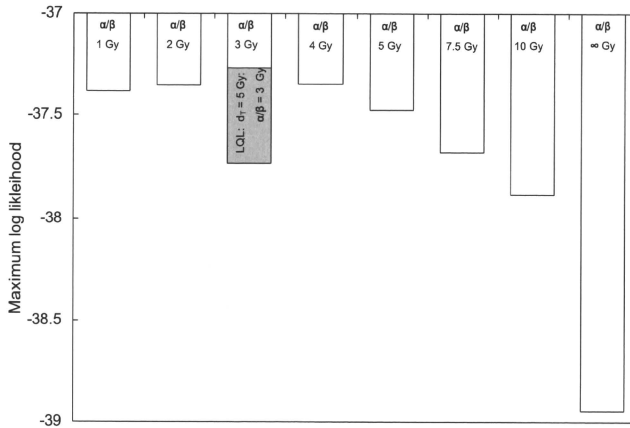


Fig. 5. The maximum log likelihood of the NTCP fit for the MLD calculated for different α/β ratios is shown. In the grey rectangle the maximum log likelihood of the NTCP fit based on the MLD calculated with the LQL model (with an α/β ratio of 3 Gy and a d_T of 5 Gy) is indicated next to the MLD_3 . The maximum log likelihood of the NTCP fit based on the MLD calculated with the LQL model (with an α/β ratio of 3 Gy and a d_T of 5 Gy) is indicated next to the MLD_3 .

Since the dose per fraction in hypofractionated RT is considerably larger than 2 Gy, a substantial volume of lung tissue received more than 2 Gy per fraction. Because the $MLDLQ$ is expressed as 2-Gy equivalents, the $MLDLQ$ is, therefore, expected to be larger than the MLD_{phys} . Evaluating different α/β ratios resulted in different relationships between the $MLDLQ$ and the MLD_{phys} . By the nature of the LQ model, for lower α/β ratios and higher fraction doses, the difference between the $MLDLQ$ and MLD_{phys} increased, and for higher α/β ratios, the $MLDLQ$ approached that of the MLD_{phys} . Because of the strong correlation between the $MLDLQ$ and the MLD_{phys} , it might be questioned whether the physical dose can be used to estimate complication probabilities. However, our results confirm also that after hypofractionation, the physical dose should not be used for calculation of toxicity probabilities.

By calculating the MLD, the local dose in the lungs is weighted according to a linear local dose-effect relation. In contrast, for the V_x , the local dose-effect relationship is considered a binary effect whereby no damage is taken into account below the threshold dose of xGy and a full damage above the threshold dose of xGy . Different dose volume parameters and their mutual relationships have not previously been evaluated for hypofractionated RT. Since the dose effect relationship expressed by the MLD and V_x are based on different parameters (*i.e.*, models are not nested), a direct comparison of the NTCP fits via a log likelihood ratio approach is not possible. Including these parameters (MLD , V_5 , V_{13} , V_{20} , and V_{40}) in a multivariate logistic regression analysis revealed that only the MLD was significantly associated with RP (data not shown). However, these data should be interpreted with caution since it is known from studies with con-

ventional fractionated RT evaluating clinical and dose factors predicting RP that there is a large heterogeneity of results (21–32), whereby no validation was performed. One collaborative study from Duke University and The Netherlands Cancer Institute developed a prospective method to predict RP from dose and clinical parameters in one group of patients, but validation failed in another group of patients (33).

The validity of the LQ model for both clonogenic cell survival as clinical isodose calculations for higher dose per fraction was discussed previously; Hall and Brenner (11) estimated from the isoeffect data of van der Kogel (34) (late-responding damage to the rat spinal cord) and Douglas and Fowler (35) (acute damage to the mouse skin) that the LQ model would be valid for single doses up to 20 Gy. According to this estimation, Fowler *et al.* (9) extrapolated the relationship between RP and MLD, as determined for conventionally treated patients, to hypofractionated schemes. Unfortunately, clinical data were lacking to validate such an extrapolation. Concerning RP (or other clinical toxicity endpoints), it might be questioned whether the applicability of the LQ model for these fraction doses can be answered by clinical studies. For example, the high number of (noncoplanar) beams results in an irradiation dose to healthy (lung) tissue that will be much smaller than the maximum dose. In addition, the relative volume of healthy tissue receiving such a high dose is limited by current advanced radiotherapy techniques (*e.g.*, intensity-modulated RT and Image guided RT [IGRT]). Moreover, the purpose of these techniques is to avoid high doses to normal tissues.

Guerrero *et al.* (5) developed a modification of the LQ model by extending the LQ model with a protraction factor, based on the lethal-potentially lethal (LPL) model, which is

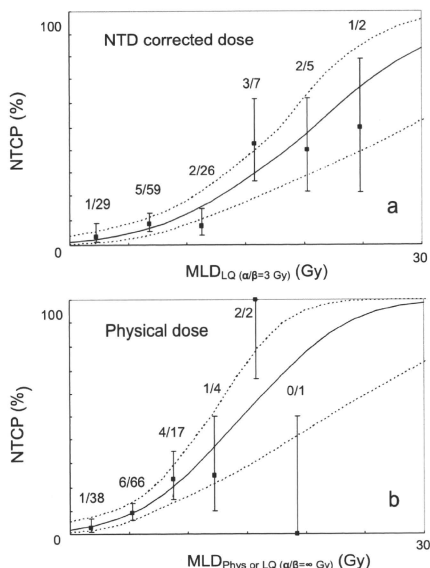


Fig. 6. (Top) The NTCP fit (solid line) is shown as a function of the MLD calculated according to the LQ model and an α/β ratio of 3 Gy with the 68% CI (dotted lines) ($TD_{50} = 20.8$ Gy, $m = 0.45$). The number of events and number of patients are indicated. (Bottom) The NTCP fit (solid line) is shown as a function of the physical MLD (*i.e.*, LQ model and an α/β ratio of infinity) with the 68% CI (dotted lines) ($TD_{50} = 14.6$ Gy, $m = 0.48$). The number of events and number of patients are indicated.

supposed to be superior, describing log cell survival data in the higher dose region (36). This modification was based on cell survival and animal toxicity data. The authors observed a wide range of dose values where the LQ started to deviate from the LPL model (cell lines 0.6 Gy to 37.7 Gy; animal toxicity data 2.6 Gy to 100 Gy). It was shown that this modification results in a LQ model with a linear extension of the log cell survival as function of the dose for the high-dose range by Carlone *et al.* (6), and they proposed to name this model the linear-quadratic-linear (LQL) model. Elaborating this discussion in the clinical setting, we evaluated the LQL model with clinical data by using the simpler but similar method proposed by Park *et al.* (4), using a linear extension of the log cell survival as a function of the dose for doses higher than the threshold (*i.e.*, transition dose d_T). For a d_T of 5 Gy, we observed a (nonsignificant) worse NTCP fit. For higher d_T values, the LQL NTCP fit approached the LQ NTCP fit; the differences between the MLDLQL and MLDLQ are becoming smaller because less lung tissue dose will be recalculated according to the linear part of the LQL model (dose larger than the d_T). Last, if the d_T is larger than the largest fraction doses, the MLDLQL equals the

Table 1. The optimized V_{x50} and m for the different V_x values with the 95% CI

V_x value	V_{x50} (95% CI)	m (95% CI)	Maximum log likelihood
V_5	65.4 (49.0–121.0) [†]	0.46 (0.34–0.66)	–39.40
V_{13}	39.2 (30.0–77.0)	0.48 (0.36–0.67)	–39.77
V_{20}	30.6 (23.0–57.0)	0.50 (0.37–0.68)	–39.63
V_{40}	15.9 (13.0–27.0)	0.48 (0.37–0.65)	–38.12
V_{50}	13.1 (11.0–21.0)	0.48 (0.37–0.65)	–37.04

The V_{x50} and m representing the value of V_x (%) with a 50% Normal Tissue Complication Probability (NTCP) and steepness parameter, respectively.

[†] Note that the upper boundary of 95% CI exceeds the 100% lung volume due to the approximation in the statistical method applied, whereas in mathematical and clinical terms, the upper limit is 100%.

MLDLQ. Another mathematical model to describe the cellular response as function of the irradiation dose is the linear quadratic cubic (LQC) (37) model, whereby the cubic term is negative. This LQC model also has a (more) linear response in the high-dose region, approximating that of the LPL model. As with the LQL model, the LQC model is mathematically simpler than the LPL model, with only one additional parameter (as in the LQL model).

At the NKI (and many other institutes), the hypofractionated schedule that is mainly given is 3×18 Gy. Unfortunately, the patients treated at the NKI could not be included in the current analysis. The first reason for this is the limited follow-up of a substantial part of these patients. Second, the patients with sufficient follow up (>1 year) had lung doses only in the lower MLD range, resulting in low incidences of RP. Consequently, these patients cannot be of additional value for this type of analysis. However, the relationship between the MLDLQL as a function of the MLDLQ for

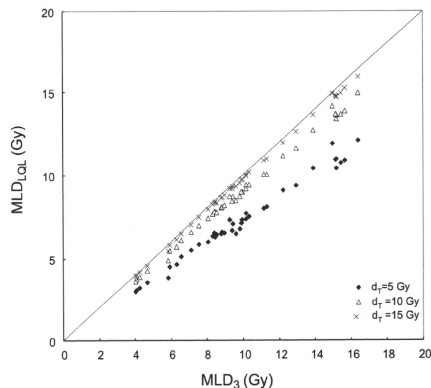


Fig. 7. For patients treated at the NKI-AVL, the MLDLQL is plotted as a function of MLD_3 for a d_T of 5 Gy, a d_T of 10 Gy, and a d_T of 15 Gy. The straight line with a slope 1 represents the equivalent line where MLDLQL equals MLD_3 .

higher transition doses than those used in current analysis could be evaluated. As illustrated in Fig. 7, only a d_T of about 10 Gy or lower results in a difference between the MLDLQ and the MLDLQ. Introduction of a higher d_T would lead to imperceptible differences between the MLDLQ and the MLDLQ. Consequently, it might be questioned whether a higher d_T can be clinically evaluated with respect to RP in the future due to limited amount of lung tissue receiving high doses. Irradiation of healthy lung tissue of animals with increasing fraction sizes, which could be possible in the future with advances in preclinical irradiation techniques, might facilitate resolving this issue.

We evaluated the LQL model by using an α/β ratio of 3 Gy, which did not improve the NTCP fit to the data. Although the slope of the linear component is dependent of both the d_T and the α/β ratio, we did not analyze the LQL model with other α/β values. The first reason for this is that evaluations of the LQL model with α/β ratios close to 3 Gy would not affect the NTCP fit significantly according to current data. Second, for (much) higher α/β values, the LQL model approaches the LQ model (for α/β equal to infinity the LQL and LQ model both are becoming the L [linear] model). Third, for lung tissue, an α/β value of 3 to 4 Gy is an accepted value, converting doses in the lower dose range (38–42).

Predictive models based on clinical data are as good as the clinical data. Consequently, the limitations of this study should be stressed. We discussed the clinical limitations of our study comprehensively previously (12). First, the study was a retrospective univariate analysis evaluating RP grade ≥ 2 . Second, although the assessment of RP was carefully performed, the prescription of steroids and oxygen relies on the intention to treat of the physician. Third, only one grade 3 RP was scored, and the duration of the RP grade 2 treatment was not registered. Therefore, no dose response analysis could be performed regarding the severity of the radiation-induced toxicity. Another discussion point is whether the time interval between the subsequent treatments should be

taken into account. As discussed previously (12), we did not consider any repair between the treatments. A mouse study suggested that for higher doses per fraction, less recovery might be expected (43). Moreover, limited clinical data showed that patients are experiencing a high probability of RP after reirradiation (44).

Besides the reliability of NTCP modeling on the robustness of the clinical data, some assumptions have to be made for (NTCP) modeling in general. First, a NTCP model based on one (dose) characteristic disregards all other factors influencing the probability to develop toxicity (e.g., genetic variability and/or comorbidity) for one individual patient. Second, to evaluate clinically applicable dose parameters, dose-volume histograms are reduced to simple parameters (e.g., MLD and V_x), whereby a (biological) background is assumed but questionable. Third, the limited number of patients included in the current study might have caused the fact that a real intrinsic difference between these parameters was not apparent with statistical significance.

CONCLUSIONS

In conclusion, with our study we provide clinical toxicity data for the discussion of the applicability of current radiobiological models for higher doses per fraction. We observed that the LQ model was valid (with an α/β ratio of 3 Gy for lung tissue) to recalculate the physical dose into biologically equivalent dose and that the biological dose should be used for estimating toxicity probabilities. The LQL model did not improve the prediction of RP. This might be due to the limitations of our study and/or to (still) unknown fundamental mechanisms complicating the translation of mathematical models developed with cell survival data into clinical data. With currently used fraction doses of up to 18 Gy, substantially different results are not expected, but this should be confirmed in future evaluations.

REFERENCES

- Fowler JF. The first James Kirk memorial lecture. What next in fractionated radiotherapy? *Br J Cancer Suppl* 1984;6:285–300.
- Tucker SL. Tests for the fit of the linear-quadratic model to radiation isoeffect data. *Int J Radiat Oncol Biol Phys* 1984;10:1933–1939.
- Puck T, Marcus P. Action of x-rays on mammalian cells. *J Exp Med* 1956;103:653–666.
- Park C, Papiez L, Zhang S, et al. Universal survival curve and single fraction equivalent dose: useful tools in understanding potency of ablative radiotherapy. *Int J Radiat Oncol Biol Phys* 2008;70:847–852.
- Guerrero M, Li XA. Extending the linear-quadratic model for large fraction doses pertinent to stereotactic radiotherapy. *Phys Med Biol* 2004;49:4825–4835.
- Carlone M, Wilkins D, Raaphorst P. The modified linear-quadratic model of Guerrero and Li can be derived from a mechanistic basis and exhibits linear-quadratic-linear behaviour. *Phys Med Biol* 2005;50:L9–L13.
- Barendsen GW. Dose fractionation, dose rate and iso-effect relationships for normal tissue responses. *Int J Radiat Oncol Biol Phys* 1982;8:1981–1997.
- Denekamp J, Waites T, Fowler JF. Predicting realistic RBE values for clinically relevant radiotherapy schedules. *Int J Radiat Biol* 1997;71:681–694.
- Fowler JF, Tome WA, Fenwick JD, et al. A challenge to traditional radiation oncology. *Int J Radiat Oncol Biol Phys* 2004;60:1241–1256.
- Hall EJ, Brenner DJ. The radiobiology of radiosurgery: Rationale for different treatment regimes for AVMS and malignancies. *Int J Radiat Oncol Biol Phys* 1993;25:381–385.
- Marks LB. Extrapolating hypofractionated radiation schemes from radiosurgery data: Regarding Hall et al., *Int J Radiat Oncol Biol Phys* 1991;21:819–824 and Hall and Brenner, *Int J Radiat Oncol Biol Phys* 1993;25:381–385. *Int J Radiat Oncol Biol Phys* 1995;32:274–276.
- Borst GR, Ishikawa M, Nijkamp J, et al. Radiation pneumonitis in patients treated for malignant pulmonary lesions with

- hypofractionated radiation therapy. *Radiother Oncol* 2009;91:307–313.
13. Semenenko VA, Li XA. Lyman-Kutcher-Burman NTCP model parameters for radiation pneumonitis and xerostomia based on combined analysis of published clinical data. *Phys Med Biol* 2008;53:737–755.
 14. Yamashita H, Nakagawa K, Nakamura N, *et al.* Exceptionally high incidence of symptomatic grade 2-5 radiation pneumonitis after stereotactic radiation therapy for lung tumors. *Radiat Oncol* 2007;2:1–11.
 15. Lebesque JV, Keus RB. The simultaneous boost technique: the concept of relative normalized total dose. *Radiother Oncol* 1991;22:45–55.
 16. Lyman JT. Complication probability as assessed from dose-volume histograms. *Radiat Res Suppl* 1985;8:S13–S19.
 17. Seppenwoolde Y, Lebesque JV, De Jaeger K, *et al.* Comparing different NTCP models that predict the incidence of radiation pneumonitis. Normal tissue complication probability. *Int J Radiat Oncol Biol Phys* 2003;55:724–735.
 18. Venzon DJ, Moolgavkar SH. A method for computing profile-likelihood-based confidence intervals. *Applied Statistics* 1988;37:87–94.
 19. Clayton D, Hills M. Statistical models in epidemiology. Oxford University Press; New York: 1993.
 20. Kwa SL, Theuws JC, Wagenaar A, *et al.* Evaluation of two dose-volume histogram reduction models for the prediction of radiation pneumonitis. *Radiother Oncol* 1998;48:61–69.
 21. Claude L, Perol D, Ginestet C, *et al.* A prospective study on radiation pneumonitis following conformal radiation therapy in non-small-cell lung cancer: Clinical and dosimetric factors analysis. *Radiother Oncol* 2004;71:175–181.
 22. Fujino M, Shirato H, Onishi H, *et al.* Characteristics of patients who developed radiation pneumonitis requiring steroid therapy after stereotactic irradiation for lung tumors. *Cancer J* 2006;12:41–46.
 23. Hernando ML, Marks LB, Bentel GC, *et al.* Radiation-induced pulmonary toxicity: a dose-volume histogram analysis in 201 patients with lung cancer. *Int J Radiat Oncol Biol Phys* 2001;51:650–659.
 24. Inoue A, Kunitoh H, Sekine I, *et al.* Radiation pneumonitis in lung cancer patients: A retrospective study of risk factors and the long-term prognosis. *Int J Radiat Oncol Biol Phys* 2001;49:649–655.
 25. Kim TH, Cho KH, Pyo HR, *et al.* Dose-volumetric parameters for predicting severe radiation pneumonitis after three-dimensional conformal radiation therapy for lung cancer. *Radiology* 2005;235:208–215.
 26. Moreno M, Aristu J, Ramos LI, *et al.* Predictive factors for radiation-induced pulmonary toxicity after three-dimensional conformal chemoradiation in locally advanced non-small-cell lung cancer. *Clin Transl Oncol* 2007;9:596–602.
 27. Oh D, Ahn YC, Park HC, *et al.* Prediction of radiation pneumonitis following high-dose thoracic radiation therapy by 3 Gy/ fraction for non-small cell lung cancer: analysis of clinical and dosimetric factors. *Jpn J Clin Oncol* 2009;39:151–157.
 28. Rancati T, Ceresoli GL, Gagliardi G, *et al.* Factors predicting radiation pneumonitis in lung cancer patients: A retrospective study. *Radiother Oncol* 2003;67:275–283.
 29. Rodrigues G, Lock M, D'Souza D, *et al.* Prediction of radiation pneumonitis by dose-volume histogram parameters in lung cancer—A systematic review. *Radiother Oncol* 2004;71:127–138.
 30. Schallenkamp JM, Miller RC, Brinkmann DH, *et al.* Incidence of radiation pneumonitis after thoracic irradiation: Dose-volume correlates. *Int J Radiat Oncol Biol Phys* 2007;67:410–416.
 31. Tucker SL, Liu HH, Liao Z, *et al.* Analysis of radiation pneumonitis risk using a generalized Lyman model. *Int J Radiat Oncol Biol Phys* 2008;72:568–574.
 32. Willner J, Jost A, Baier K, *et al.* A little to a lot or a lot to a little? An analysis of pneumonitis risk from dose-volume histogram parameters of the lung in patients with lung cancer treated with 3-D conformal radiotherapy. *Strahlenther Onkol* 2003;179:548–556.
 33. Kokac Z, Borst GR, Zeng J, *et al.* Prospective assessment of dosimetric/physiologic-based models for predicting radiation pneumonitis. *Int J Radiat Oncol Biol Phys* 2007;67:178–186.
 34. van der Kogel AJ. Chronic effects of neutrons and charged particles on spinal cord, lung, and rectum. *Radiat Res Suppl* 1985;8:S208–S216.
 35. Douglas BG, Fowler JF. The effect of multiple small doses of x rays on skin reactions in the mouse and a basic interpretation. *Radiat Res* 1976;66:401–426.
 36. Curtis SB. Lethal and potentially lethal lesions induced by radiation—A unified repair model. *Radiat Res* 1986;106:252–270.
 37. Joiner MC. Quantifying cell kill and cell survival. In: van der Kogel AJ, Joiner MC, editors. Basic clinical radiobiology, 4th ed. Hodder Arnold, London, UK; 2009. p. 42–55.
 38. Fowler JF. The linear-quadratic formula and progress in fractionated radiotherapy. *Br J Radiol* 1989;62:679–694.
 39. Kwa SL, Lebesque JV, Theuws JC, *et al.* Radiation pneumonitis as a function of mean lung dose: An analysis of pooled data of 540 patients. *Int J Radiat Oncol Biol Phys* 1998;42:1–9.
 40. Thames HD, Bentzen SM, Turesson I, *et al.* Time-dose factors in radiotherapy: A review of the human data. *Radiother Oncol* 1990;19:219–235.
 41. Van Dyk J, Mah K, Keane TJ. Radiation-induced lung damage: Dose-time-fractionation considerations. *Radiother Oncol* 1989;14:55–69.
 42. Bentzen SM, Joiner MC. The linear-quadratic approach in clinical practice. In: van der Kogel AJ, Joiner MC, editors. Basic clinical radiobiology, 4th ed. Hodder Arnold; 2009. p. 120–134.
 43. Terry NH, Tucker SL, Travis EL. Residual radiation damage in murine lung assessed by pneumonitis. *Int J Radiat Oncol Biol Phys* 1988;14:929–938.
 44. Okamoto Y, Murakami M, Yoden E, *et al.* Reirradiation for locally recurrent lung cancer previously treated with radiation therapy. *Int J Radiat Oncol Biol Phys* 2002;52:390–396.

